Development of a Converter Based Microgrid Test Platform

Dingrui Li[1], Yiwei Ma[1], Chengwen Zhang[1], He Yin[1], Ishita Ray[1], Yu Su[1], Lin Zhu[1], Fred Wang[1,2], and Leon M. Tolbert [1,2]

[1] Min H. Kao Department of Electrical Engineering & Computer Science,
The University of Tennessee, Knoxville, TN, USA
[2]Oak Ridge National Laboratory, Knoxville, TN, USA

dli35@vols.utk.edu

***Abstract*— To overcome the limitations of digital simulation (numerical oscillation, limited computing capability of processors, etc.), a converter-based hardware test-bed was developed at CURENT for real-time power grid emulation. However, distribution systems especially microgrids cannot be emulated and tested on the existing hardware test-bed. This paper develops a microgrid test-bed based on the existing hardware test-bed to enable controller testing for microgrids with dynamic boundary. The design and realization of the microgrid hardware test-bed are introduced. The experimental results of the microgrid controller tests are also provided.**

Keywords—Microgrid, hardware test-bed, emulation, dynamic boundary

I. INTRODUCTION

Since power converters can emulate different power grid components, a DC-link shared, down-scaled, converter based emulation system called hardware test-bed (HTB) has been built at Center for Ultra-Wide-Area Resilient Electric Energy Transmission Networks (CURENT) for electric power system tests [1]. HTB is a power hardware emulation platform with several advantages. First, compared with pure digital simulations or hardware in-the-loop (HIL) tests, HTB is a physical platform that takes into consideration more practical issues such as measurement errors, communication time delays, actual power flow, etc., without requiring extra computational resources. Numerical oscillations caused by the discontinuities or interpolation in digital simulation can also be avoided in HTB testing. In addition, compared with actual systems, HTB can be easily adapted for emulation of systems with various topologies.

HTB has demonstrated its capability of transmission level emulation in several application cases. A voltage stability assessment method and a control strategy for transmission system have been tested on HTB in [2]. In references [3] and [4], HTB is used to test a measurement-driven oscillation damping control in transmission systems. However, the HTB is not capable of emulating distribution systems, especially microgrids. In order to realize microgrid tests, further development is needed on the existing HTB.

Microgrids are composed of diverse components including generators, loads, distributed energy resources (DERs), etc. In digital simulations, in order to get an accurate model for each component, several critical and practical factors (delays, measurement errors, non-linearity, etc.) should be taken into consideration. If all the practical factors were considered for all the components in microgrids, the models would become extremely complex and cause heavy computational burden. Therefore, to improve computational efficiency without compromising test accuracy, hardware emulation is a commonly used method in microgrid tests [5-7]. Reference [5] applied power hardware in-the-loop (PHIL) test on a microgrid with complex communication network. Reference [6] did the PHIL microgrid test for real hardware response. Reference [7] tested a microgrid reconnection control strategy on a hardware emulation platform with large distribution generator emulators. Hardware emulation and test serve an important role in the development of microgrids, especially, with complex configurations. DC-link shared HTB is a converter-based hardware emulation platform. It is able to emulate the whole grid with low active power requirement, and is flexible to emulate different topologies. Therefore, developing this test-bed can facilitate potential tests for other microgrids, especially the ones that require the capability of topology variations.

In this paper, a converter based microgrid HTB is developed. The microgrid in [8] is used as an example to realize the microgrid test in HTB. The microgrid in [8] is able to operate with dynamic boundary and will be implemented in the field. Functions of the microgrid controller have been tested and debugged with the proposed microgrid test-bed.

The structure of this paper is organized as follows: Section II introduces the existing HTB, followed by Section III, which describes the microgrid HTB development. The controller test design and results on HTB are given in Section IV. Section V concludes the paper.

II. Existing HTB Implementation

A. HTB Converter Emulation

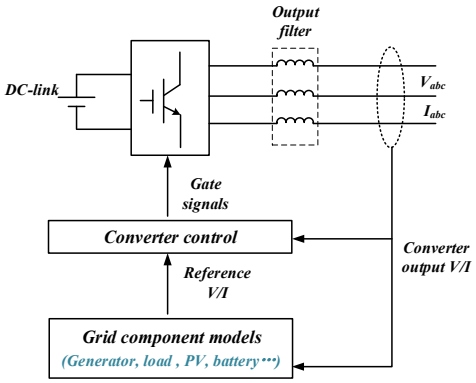

Fig. 1. Converter emulation structure

In the existing HTB, converters are applied as the emulators to emulate different grid components. The converter emulation structure is shown in Fig. 1 [9]. Each converter emulates the electrical characteristics of one grid component. Converter voltage/current references are calculated by the grid component models. The calculated references are tracked by the converter controllers. In the existing HTB, different grid components have been emulated, including generators [10], PVs [11], induction motor loads [12], batteries [13], etc.

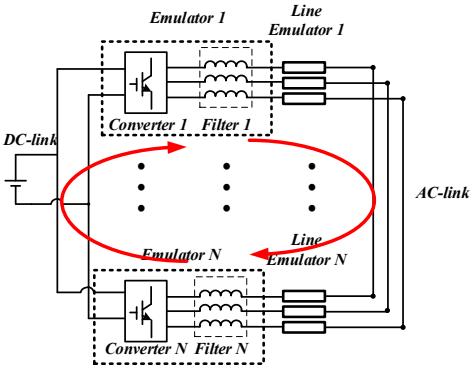

Fig. 2. HTB Structure [9]

B. HTB Hardware Structure

Converter emulators in the HTB have a paralleled connection structure which is shown in Fig. 2. All the converters share the same DC-link and different grid topologies are realized by different AC-link connections. AC lines are modelled by series inductance and resistance and emulated by inductors [14]. Due to the parallel structure, the real power circulates among converters and the platform requires low power from the grid. Meanwhile, the circulating zero-sequence current issues caused by the parallel structure have been solved in [15].

C. HTB Control Architecture

The control architecture of CURENT's HTB is shown in Fig. 3. Converter emulators are controlled using CompactRIOs (cRIOs) from National Instruments. The cRIOs are programmed and controlled by the desktops. Operation commands are issued by desktops to cRIOs. cRIOs send the commands to the converter controllers (DSP) to calculate references and obtain the AC link terminal measurements. These terminal measurements are sent from cRIOs to the desktops on a visualization wall (a 3 × 5 array of displays).

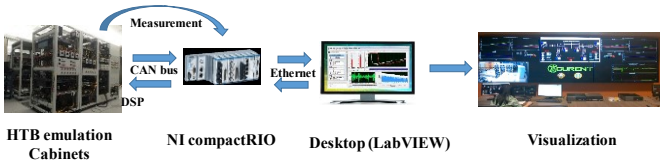

Fig. 3. HTB control architecture

III. Microgrid HTB Development

A. Microgrid HTB Test Design

1) Microgrid topology

The topology of the microgrid discussed in [8] is used for microgrid HTB development. It comes from an actual 12.8 kV, 1 MW radial system. In the HTB test, the microgrid topology in [8] is simplified to seven loads, two grid interfaces, one PV and one battery. The topology is shown in Fig. 4. The distribution line is modeled as a series resistance and inductance. This microgrid has a dynamic boundary. Dynamic boundary is the capability that enables the microgrid to pick up or shed load when the DER generation and/or storage outputs change so that the microgrid boundary can be expanded or shrunk. The boundary change is shown in Fig. 4.

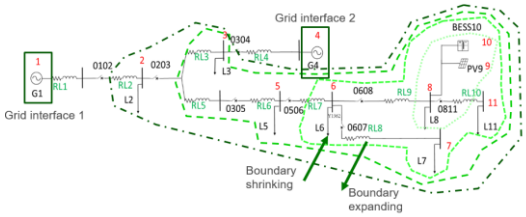

Fig. 4. Microgrid topology

2) Microgrid control architecture

The control architecture of the microgrid is also introduced in [8], which is shown in Fig. 5. The microgrid central controller communicates with the SCADA systems to control the local controllers as well as the smart switches. Several functions which enable the dynamic boundary capability have been implemented in the microgrid central controller, including

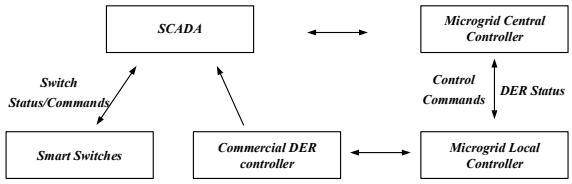

Fig. 5. Microgrid control architecture

online topology assessment, active/reactive power balance, synchronization, etc. The detailed description of these functions are stated in [8].

3) Microgrid controller HTB test architecture design

The controllers discussed in [8] are implemented in the cRIOs. Based on the existing HTB architecture, an actual microgrid controller in-the-loop test is designed. The architecture is shown in Fig. 6.

The loads and DERs in the microgrid are emulated by converters. Load emulators are directly controlled by the microgrid control panel through the HTB control desktops. The DER emulators are controlled by the microgrid local controllers. The microgrid boundary controller controls the smart switch emulators and gets the measurements from the microgrid. The local controllers and boundary controller are interact with the microgrid central controller.

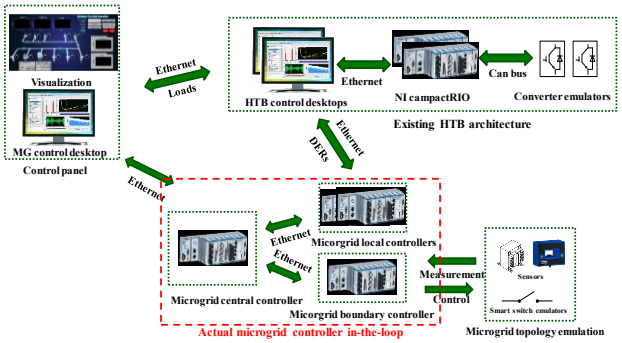

Fig. 6. Microgrid controller in-the-loop test architecture

B. Microgrid Test-bed Implementation

CURENT's HTB has shown numerous capabilities for transmission level system emulation. However, distribution systems, especially microgrids could not previously be emulated on the existing HTB. Here are several reasons:

- Battery emulators only have grid-following mode control strategy.
- Lack of reconfiguration capability among different types of systems.
- Improper line impedance value for emulating distribution systems on a per unit basis.

All the mentioned limitations are solved to realize microgrid emulation, and are described in the following.

1) Battery emulator control strategy

For the battery emulator, the control strategy in [13] only achieved battery emulation in the grid-following mode while the microgrid requires the battery with both grid-following and grid-forming capabilities. The battery emulator control strategy is shown in Fig. 7.

There are 3 modes in the battery local controllers which are (1) grid-forming mode, (2) grid-following mode and (3) local grid-forming mode. The grid-forming mode works when the microgrid operates in the islanded mode, where the battery works as the microgrid source. The grid-following mode takes over when the microgrid operates in the grid-connected mode. The local grid forming mode is designed for the islanding transition.

Since the communication from the microgrid central controller to local controller have delay or abnormal conditions, it is possible that the grid is disconnected from the battery emulator while the battery still works in the grid-following mode. In this case, the battery will reach the local grid-forming mode when the battery emulator locally detects the abnormal voltage or frequency. The battery will change from the local grid-forming mode to the normal grid-forming mode when the grid-forming-enable command from the central controller arrives.

The differences between normal grid-forming mode and local grid-forming mode is that the local grid-forming mode

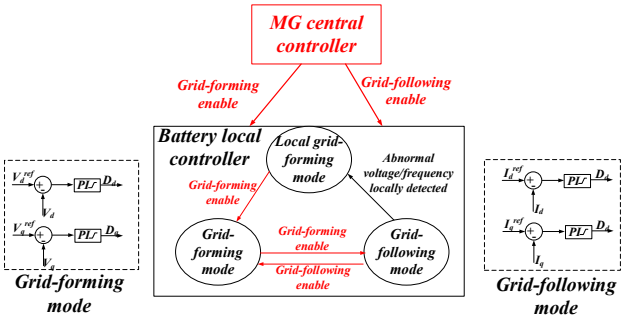

Fig. 7. Battery emulator control strategy

cannot switch back to the grid-following mode to reduce the influences of the communication error during islanding transition.

2) Reconfiguration capability

The developed microgrid HTB is designed to be reconfigurable for both transmission system (TS) and microgrid (MG) tests. The reconfigured design is shown in Fig. 8. Isolation switches are added on the AC link to switch between different test systems. In addition, by changing the MG isolation switch connections, the proposed microgrid HTB is

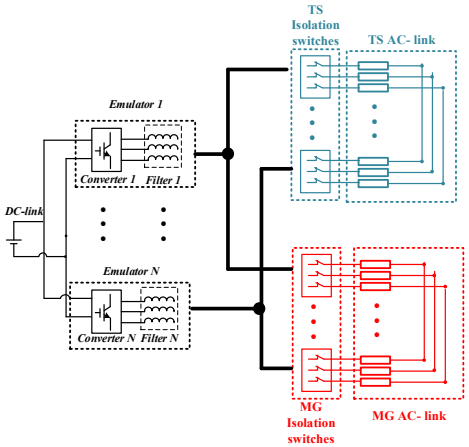

Fig. 8. HTB reconfiguration design

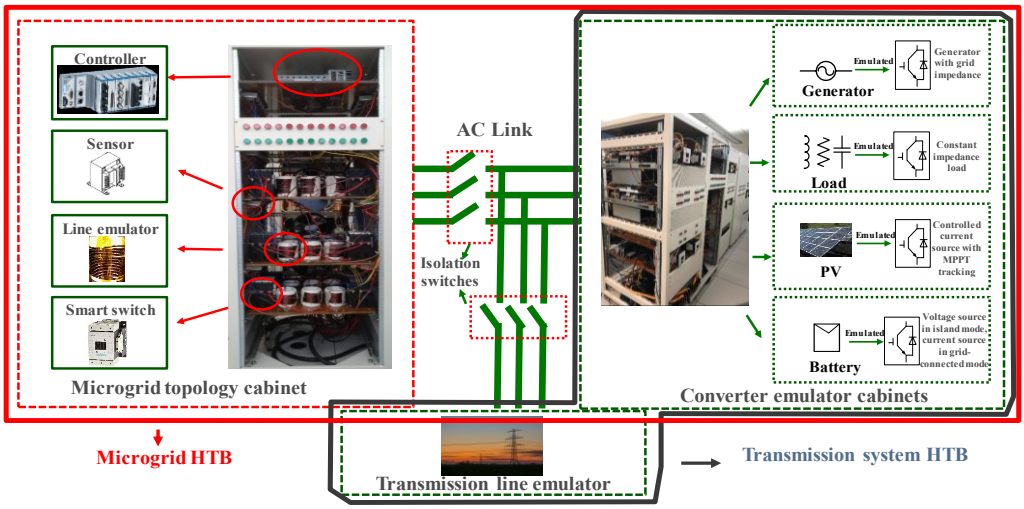

Fig. 9. Microgrid Test platform hardware implementation

able to emulate different microgrid topologies. When both MG and TS isolation switches are open, HTB is available for other applications, which keeps the flexibility of the HTB for further applications.

3) Microgrid line emulation

The microgrid HTB is designed as a 173 V and 3 kW rated system for per unit implementation. The original and rescaled line impedance values are shown in TABLE I. Compared with the line parameters in existing HTB [1], the microgrid line impedance values are much smaller. In the developed microgrid HTB, air-core inductors are applied to emulate the low-impedance microgrid lines. Three single phase inductors are grouped together as a three phase inductor. Compared with the magnetic-core inductors, the air-core inductors are lighter, easier to realize and will not saturate.

TABLE I. Microgrid line impedance

Name		Original (1MW, 12.8 kV)	Rescaled (3 kW, 173V)
RL1	R1	0.0002 p.u	2.0 (mΩ)
	L1	0.00197 p.u	19.7 (μH)
RL2	R2	0.00087 p.u	8.7 (mΩ)
	L2	0.00854 p.u	85.4 (μH)
RL3	R3	0.00013 p.u	1.3 (mΩ)
	L3	0.00093 p.u	9.3 (μH)
RL4	R4	0.00057 p.u	5.7 (mΩ)
	L4	0.00375 p.u	37.5 (μH)
RL5	R5	0.00022 p.u	2.2 (mΩ)
	L5	0.00146 p.u	14.6 (μH)
RL6	R6	0.00023 p.u	2.3 (mΩ)
	L6	0.00103 p.u	10.3 (μH)
RL7	R7	0.00088 p.u	8.8 (mΩ)
	L7	0.00379 p.u	37.9 (μH)
RL8	R8	0.00006 p.u	0.6 (mΩ)
	L8	0.00023 p.u	2.3 (μH)
RL9	R9	0.00688 p.u	68.8 (mΩ)
	L9	0.0011 p.u	11.1 (μH)
RL10	R10	0.00552 p.u	55.2 (mΩ)
	L10	0.00555 p.u	55.5(μH)

4) Overall test-bed realization

The microgrid HTB hardware implementation is shown in Fig. 9. The microgrid topology cabinet emulates the topology in Fig. 4. Microgrid controllers, sensors, line emulators and smart switch emulators are included in this cabinet. The smart switches are emulated by the contactors to realize the microgrid dynamic boundary capability. The contactors have 20-95 ms opening delay as well as 40-60 ms closing delay. Therefore, this microgrid HTB is capable of testing the impact of switching action delay. All the converter emulators are connected to the topology cabinet through the isolation switches to realize the reconfiguration capability.

IV. Test Design and Results

The controller of the microgrid in [8] has been tested on the developed HTB. Five test scenarios have been designed and tested, which include black start, steady-state islanded operation, reconnection, islanding and steady-state grid connected operation with dynamic boundary.

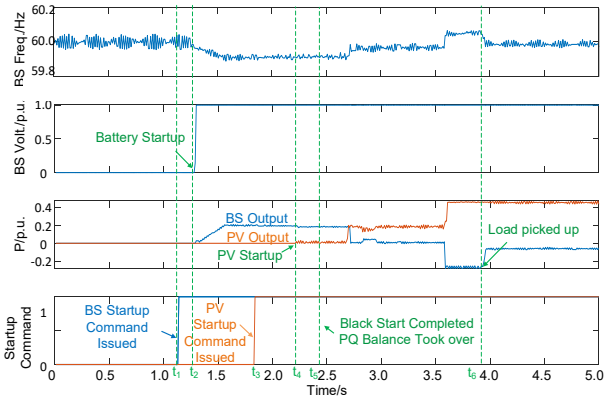

Fig.10. Experimental results of black start

A. Black Start

Black start is the process where the PV and battery start to pick up the loads and lead the microgrid to the islanded mode. The test results are shown in Fig 10. The microgrid controller issues the battery and PV startup command at t_1 and t_4. The battery and PV completes their individual startup at t_2 and t_4, respectively. The black start is completed at t_5, and the loads starts to be picked up at t_6.

B. Steady-State Islanded Operation

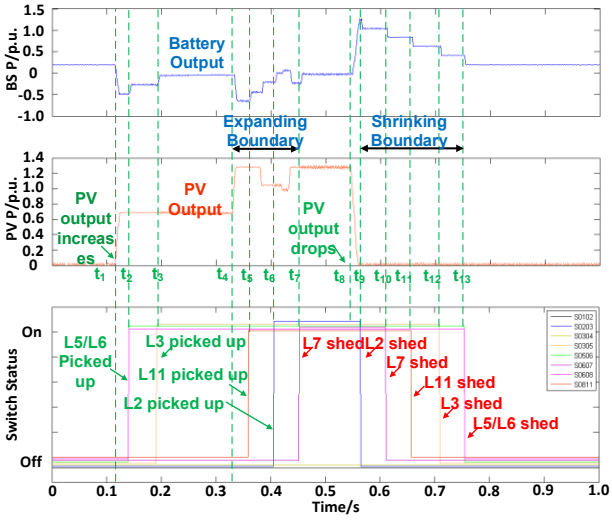

Fig.11. Steady-state islanding operation

For this test case, the microgrid operates in the islanded mode with power balance and is able to pick up or shed load to change the microgrid boundary when the PV output changes. The test results are shown in Fig 11. In the steady state islanded test, as PV output increases, the microgrid starts to pick up loads and expands the boundary at t_1. All the loads are picked up at t_7. At t_8, as PV output decreases, the microgrid starts to disconnect the load and shrinks the boundary until all the loads are shed at t_{13}.

C. Reconnection

Reconnection is the transition from islanded mode to grid-connected mode. In the developed HTB, the reconnection can be realized through different switches. During this transition, the microgrid controller regulates the voltage differences between two sides of the boundary switch to minimize the transient current. The reconnection at switch 0608 is shown in Fig. 12.

During this reconnection, grid (G1) is enabled at t_1 and gradually picks up loads (L_2, L_3, L_6, L_7) through $t_2 - t_5$. Switch 0608 is identified as the boundary when load L_6 is picked up at t_4. Then the voltage difference information on 0608 is sent to the microgrid controller for resynchronization. After the voltage is reduced, the switch 0608 is closed at t_6, and the battery changes the control mode from grid-forming to grid-following at t_7. At t_8, the grid picks up the last load L_{11}.

During this transition, the communication delay is emulated by the developed HTB. The switching action happens at t_6 while the battery modes changes at t_7. The time between t_6 and t_7 is the delay between switching action and communication. Fluctuations in the battery current have been observed, which is realistic but rarely modeled in digital simulations.

D. Islanding

Islanding is the transition from grid-connected mode to islanded mode. In actual microgrids, there are two kinds of islanding events. The first one is planned islanding which usually happens during the grid equipment maintenance.

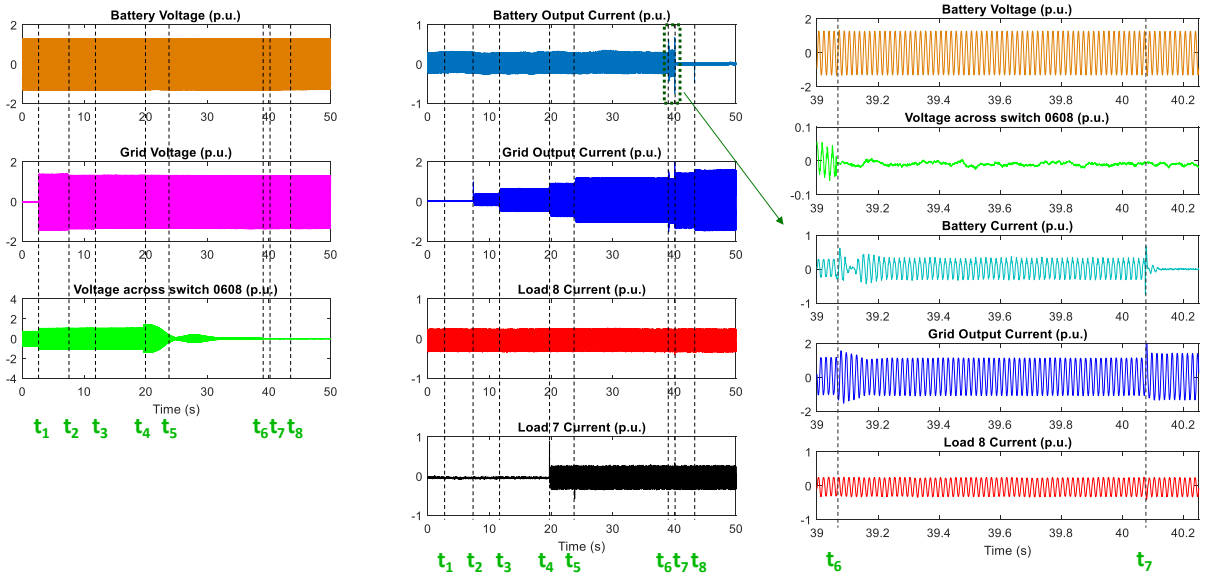

Fig. 12. Reconnection test results

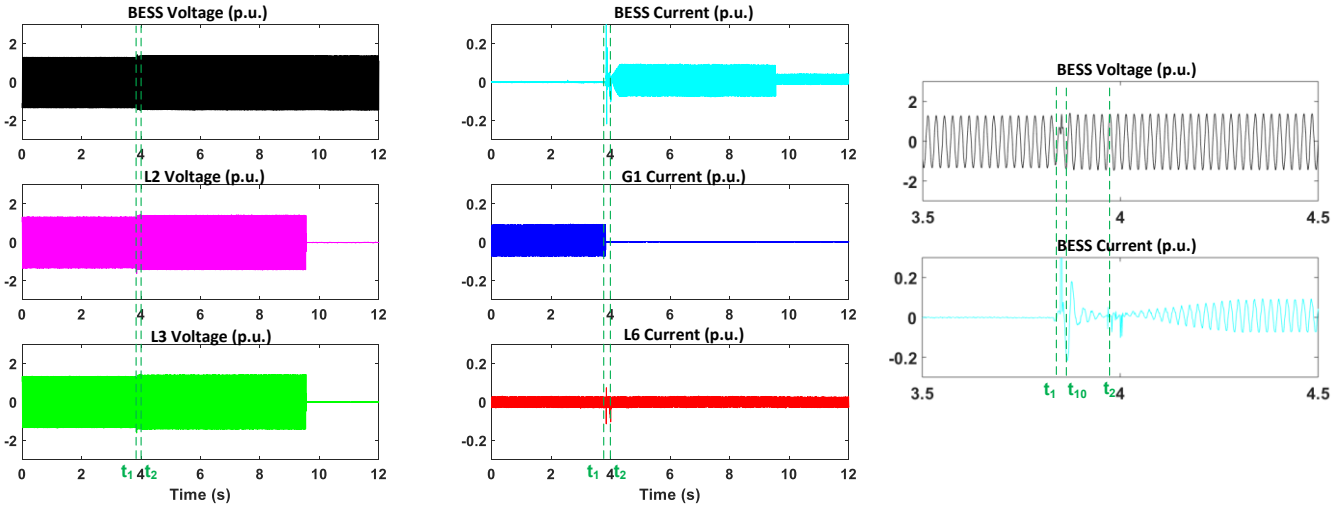

Fig. 13. Unplanned islanding test results

Planned islanding is a foreseeable islanding, and the microgrid controller can shed loads and curtail the PV and battery outputs to minimize current through the point of common coupling prior to islanding. The second is unplanned islanding, which usually results from grid fault or abnormal conditions. In the unplanned islanding case, the grid and microgrid experience large transient, which justifies pretest and emulation for determining the potential issues. Therefore, the unplanned islanding tests are covered, and the results are shown in Fig. 13.

Unplanned islanding is tested on grid G1. In this test, the unplanned islanding is tiggered manually. In the real grid, the unplanned islanding can be caused by faults. G1 became unavailable at t_1 and the microgrid reaches the steady-state islanded operation at t_2. The time between t_1 and t_2 reflects the transient of islanding. Similar to the reconnection, the delay caused by the switching action and communication has also been well emulated in the developed HTB. At t_1, the boundary switch opens while the battery emulator still operates in grid-following mode until the battery local controller detects the abnormal conditions and changes mode to the local grid-forming mode (in Fig 7) at t_{10}. The mode change command from the central controller arrives at t_2, and the battery emulator changes to the normal grid-forming mode at t_2 when the microgrid reaches the islanding operation.

E. Grid-connected Operation with Dynamic Boundary

During the steady state grid-connected operation, the microgrid operates in the grid connected mode with power balance and has the dynamic boundary capability. The test results are shown in Fig. 14. During this test, the microgrid starts from the grid-connected operation with G1. Islanding happens at t_1. Between t_1 and t_2, the microgrid goes through the islanding operation. The reconnection to grid G_4 starts at t_2 when grid G4 is enabled and starts to pick up the loads. The reconnection completes at t_3. After t_3, the microgrid operates in the grid-connected mode with grid G4.

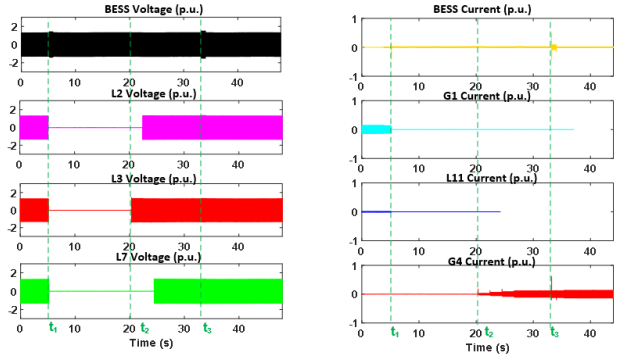

Fig. 14. Grid-connected operation with dynamic boundary test results

All the mentioned test cases demonstrate that the developed microgrid test platform is capable of emulating steady state as well as the transient microgrid operation. Based on these tests, the controller functions of dynamic boundary and the microgrid in [8] are tested and debugged. The HTB test checks the microgrid controller capabilities by considering actual power flow, time delays, etc., which is more realistic compared with the digital simulations. After the HTB test, this microgrid controller will be implemented in the actual field in the future.

V. Conclusions

The developed HTB is a new micorgrid emulation platform which is capable of emulating microgrid operation transients and practical factors. A microgrid controller with dynamic boundary has been tested and debugged on this platform through five different test cases to show HTB's capability of performing microgrid tests.

However, there are still several capabilities that can be developed in the microgrid HTB, including unbalanced load emulation, fault emulation, grid protection, etc., which are also

important in microgrid emulation. These functions will be discussed in the future.

ACKNOWLEDGMENT

This work was supported primarily by the Advanced Research Projects Agency – Energy (ARPA-E) under Award No. DE-AR0000665. This work also made use of Engineering Research Center Shared Facilities supported by the Engineering Research Center Program of the National Science Foundation and DOE under NSF Award Number EEC1041877 and the CURENT Industry Partnership Program.

The authors also would like to thank partners including Montie Smith, Jingxin Wang, Nattapat Praisuwanna and Evan McKee from CURENT at the University of Tennessee, Knoxville.

REFERENCES

[1] L. Yang, Y. Ma, J. Wang, J. Wang, X. Zhang, L. M. Tolbert*, et al.*, "Development of converter based reconfigurable power grid emulator," in *Proc*. *IEEE Energy Conversion Congress and Exposition (ECCE)*, 2014, pp. 3990-3997.

[2] F. Hu, L. Yang, J. Wang, Y. Ma, K. Sun, L. M. Tolbert, and F. Wang, "Measurement-based voltage stability assessment and control on CURENT hardware test bed system," in *Proc. IEEE PES General meeting (PESGM)*, 2016, pp. 1-5.

[3] L. Zhu, H. Liu, Y. Ma, Y. Liu, E. Farantatos, M. Patel, and S. McGuinness, "Adaptive and coordinated oscillation damping control using measurement-driven approach," in *Proc. Power Systems Computation Conference (PSCC)*, 2016, pp. 1-7.

[4] F. Bai, L. Zhu, Y. Liu, X. Wang, K. Sun, Y. Ma, M. Patel, E. Farantatos, and N. Bhatt, "Design and implementation of a measurement-based adaptive wide-area damping controller considering time delays," *Electric Power Systems Research*, vol. 130, pp. 1-9, 2016.

[5] F. Guo, L. Herrera, M. Alsolami, H. Li, P. Xu, X. Lu*, et al.*, " Design and development of a reconfigurable hybrid microgrid testbed, " in *Proc. IEEE Energy Conversion Congress and Exposition (ECCE)*, 2013, pp. 1350-1356.

[6] D. Shi, Y. Luo, and R. K. Sharma, "Active synchronization control for microgrid reconnection after islanding," in *Proc. IEEE PES Innov. Smart Grid Technol. Conf. Europe (ISGT-Europe)*, Istanbul, Turkey, 2014, pp. 1–6.

[7] J. Wang, Y. Song, W. Li, J. Guo, and A. Monti, "Development of a universal platform for hardware in-the-loop testing of microgrids, " *IEEE Transactions on Industrial Informatics,* vol. 10, pp. 2154-2165, 2014.

[8] Y. Ma, X. Hu, H. Yin, L. Zhu, Y. Su, F. Wang*, et al.*, "Real-time control and operation for a flexible microgrid with dynamic boundary, " in Proc. *IEEE Energy Conversion Congress and Exposition (ECCE)*, 2018, pp. 5158-5163.

[9] Y. Ma, J. Wang, F. Wang, and L. M. Tolbert, "Converter-based reconfigurable real-time electrical system emulation platform," *Chinese Journal of Electrical Engineering,* vol. 4, no. 1, pp. 20-27, 2018.

[10] L. Yang, J. Wang, Y. Ma, J. Wang, X. Zhang, L. M. Tolbert*, et al.*, "Three-phase power converter-based real-time synchronous generator emulation, " *IEEE Transactions on Power Electronics*, vol. 32, pp. 1651-1665, 2017.

[11] W. Cao, Y. Ma, J. Wang, L. Yang, J. Wang, F. Wang*, et al.*, "Two-stage PV inverter system emulator in converter based power grid emulation system, " in *Proc*. *IEEE Energy Conversion Congress and Exposition (ECCE)*, 2013, pp. 4518-4525.

[12] J. Wang, Y. Ma, L. Yang, L. M. Tolbert, and F. Wang, "Power converter-based three-phase induction motor load emulator, " in *Proc*. *IEEE Applied Power Electronics Conference and Exposition (APEC)*, 2013, pp. 3270-3274.

[13] J. D. Boles, Y. Ma, W. Cao, L. M. Tolbert, and F. Wang, "Battery energy storage emulation in a converter-based power system emulator, " in *Proc*. *IEEE Applied Power Electronics Conference and Exposition (APEC)*, 2017, pp. 2355-2362.

[14] S. Zhang, B. Liu, S. Zheng, Y. Ma, F. Wang, and L. M. Tolbert, "Development of a converter-based transmission line emulator with three-phase short-circuit fault emulation capability," *IEEE Transactions on Power Electronics*, vol. 33, pp. 10215-10228, 2018.

[15] Y. Ma, L. Yang, J. Wang, X. Shi, F. Wang, and L. M. Tolbert, "Circulating current control and reduction in a paralleled converter testbed system," in *Proc*. *IEEE Energy Conversion Congress and Exposition (ECCE)*, Sep. 2013, pp. 5426–5432.